AIMS Mathematics

AIMS Mathematics, 8(9): 19950–19970.
DOI: 10.3934/math.20231017
Received: 23 March 2023
Revised: 23 May 2023
Accepted: 06 June 2023
Published: 15 June 2023

http://www.aimspress.com/journal/Math

Research article

Effective transform-expansions algorithm for solving non-linear fractional multi-pantograph system

Ahmad Qazza[1], Rania Saadeh[1,*], Osama Ala'yed[2] and Ahmad El-Ajou[3]

[1] Department of Mathematics, Faculty of Science, Zarqa University, Zarqa 13110, Jordan
[2] Department of Mathematics, Jadara University, Irbid 21110, Jordan
[3] Department of Mathematics, Faculty of Science, Al Balqa Applied University, Salt 19117, Jordan

* **Correspondence:** Email: rsaadeh@zu.edu.jo.

Abstract: This study presents a new and attractive analytical approach to treat systems with fractional multi-pantograph equations. We introduce the solution as a rapidly-converging series using the Laplace residual power series technique. This method controls the range of convergence and can be easily programmed to find many terms of the series coefficients by computer software. To show the efficiency and strength of the proposed method, we compare the results obtained in this study with those of the Homotopy analysis method and the residual power series technique. Furthermore, two exciting applications of fractional non-homogeneous pantograph systems are discussed in detail and solved numerically. We also present graphical simulations and analyses of the obtained results. Finally, we conclude that the obtained approximate solutions are very close to the exact solutions with a slight difference.

Keywords: Caputo fractional derivative; multi-pantograph equations; Laplace residual power series method
Mathematics Subject Classification: 26A33, 34K37, 40G10

1. Introduction

Recently, fractional differential or integral equations and their applications have attracted great interest due to their significant role in describing and justifying various phenomena, for example, chaos synchronization, mechanical systems, image processing, earthquake modeling, wave propagation phenomena, control theory [1–5], artificial intelligence, machine learning, and deep learning in different branches of science and engineering [6,7]. In addition, systems of fractional differential equations (DEs) are a suitable tool for modeling nonlinear dynamical systems [8,9]. The fractional delay DEs are thought to be a potent tool for modeling a variety of natural phenomena, such as the model of HIV infection [10], fractional-order chaotic delayed systems [11], some automatic control systems with feedback [12], etc.

Delay DEs have various applications in different fields, such as industrial, biological, chemical, electronic and transport systems [13–16]. One of the most common types of delay DEs is the pantograph equation, which was used by Ockendon and Tayler [15] to study the collection of electric current via an electric locomotive pantograph, hence the name. The pantograph equation is given by the following DE:

$$\rho'(\tau) = \varphi\big(\tau, \rho(\tau), \rho(\delta\tau)\big), \tau \geq 0, \;\; \rho(0) = \omega,$$

where $0 < \delta < 1, m = 1, 2, \cdots, k.$
The multi-pantograph differential equation [17–19], which is an extension of the pantograph equation and has the following form:

$$\rho'(\tau) = \varphi\big(\tau, \rho(\tau), \rho(\delta_1\tau), \rho(\delta_2\tau), \cdots, \rho(\delta_k\tau)\big), \tau \geq 0, \qquad \rho(0) = \omega,$$

where $0 < \delta_m < 1, m = 1, 2, \cdots, k$, has many applications in electrodynamics, number theory, astrophysics, control of ships, probability theory, physics, engineering, economics, chemistry, nonlinear dynamical systems, cell growth, chemical kinetics, electronic systems, infectious diseases, medicine, control problems and quantum mechanics [10–16, 20–22]. The multi-pantograph differential equation involves a system with a temporal delay, and the behavior of the known variable at any given point in the previous states dictates how the unknown variable will behave.

Widatalla and Koroma [16] and other researchers [23–25] proposed the following system of multi-pantograph equations and gave an approximate solution to it by different methods:

$$\rho_r'(\tau) = \sigma_r\rho_r(\tau) + \varphi_r\left(\tau, \rho_i(\tau), \rho_j\big(\gamma_j\tau\big)\right), \qquad \rho_r(0) = \omega_r, \;\; r = 1, 2, 3 \;\cdots, m,$$

where i and $j \in \{1, 2, 3 \;\cdots, m\}$, ω_r, $\sigma_r, \gamma_j \in \mathbb{R}$, such that $0 < \sigma_r < 1$, and φ_r are functions of $\tau, \rho_i(\tau)$, and $\rho_j\big(\gamma_j\tau\big)$. This system is considered one of the most important kinds of delay DEs that can describe various kinds of applications in engineering, physics and pure and applied mathematics, such as electronic systems, quantum mechanics and dynamical systems among others.

Because many natural phenomena involve information from the past or memory, researchers saw the use of the fractional derivative as a tool to study the phenomenon in the moments leading up to the moment of its onset [26–34]. Thus, the fractional delay DEs are originally classical DEs that are reformulated by substituting the fractional derivative instead of the classical one for the abovementioned purpose. Therefore, the authors in [35–37] reformulated the above system by replacing the classical derivatives with fractional derivatives in the Caputo sense as follows and introduced approximate solutions to it through various methods:

$$D^\alpha\rho_r(\tau) = \sigma_r\rho_r(\tau) + \varphi_r\left(\tau, \rho_i(\tau), \rho_j\big(\gamma_j\tau\big)\right), \tag{1}$$

subject to

$$\rho_r(0) = \omega_r, \;\; r = 1, 2, 3 \;\cdots, m, \tag{2}$$

where $D^\alpha, \alpha \in (0,1]$ is the Caputo-fractional derivative operator, and as with all models of fractional equations, the fractional derivative describes the motion memory in the system and provides an exceptional understanding of the behavior of various dynamical systems.

Unfortunately, for the fractional multi-pantograph system (FMPS), like the different fractional models, it is difficult to provide an exact solution, and it may be impossible most of the time. Therefore, researchers resort to providing approximate solutions using analytical or numerical methods. Lately, many scholars have extensively researched and proposed numerous analytical and numerical approaches to investigate solutions of fractional equations, such as the variational iteration method [38], reproducing kernel method [39], Adomian decomposition method [40], fractional difference method [41], Homotopy perturbation method [42], Homotopy analysis method [35,43], sine-Gordon expansion method [44], artificial neural network methods [45], gradient-based optimization approach [36], fractional differential transform method [37], residual power series technique (RPST) [35,46,47] and other methods [48,49].

The RPST is an effective analytical method to set the power series solution coefficients for the ordinary and partial DEs. It is based on creating a series solution for numerous linear and nonlinear DEs and provides a convergent series solution without the need for linearization, discretization, or perturbation. Although old-fashioned, the Laplace transform (LT) is still used to solve various classes of linear DE [49]. Unfortunately, it cannot be utilized directly to solve nonlinear DE. Some analytical methods have been modified by exploiting the Laplace transform to simplify its working mechanisms, such as the Laplace Homotopy perturbation [26], Laplace Adomian decomposition method [27], Laplace Homotopy analysis method [28] and He-Laplace method [29].

Recently, on the same approach, El-Ajou and his research team employed the LT in the RPST to simplify the tactic of determining the series solution coefficients for some DEs of fractional order, such as the nonlinear time-fractional dispersive PDEs, Lane-Emden equations, multi-dimensional time-fractional Navier-Stokes system, Fisher's equation and logistic system model among others [30–34]. This employment led to the facilitation and acceleration of determining the coefficients process compared with the RPST. The new approach is called the Laplace residual power series technique (LRPST). The mechanism of the new technique depends on transforming the equation into a Laplace space and then creating a series solution for the new equation. Due to the properties of the LT, the series solution is in the form of the fractional Laurent series [30]. Series coefficients are determined using the concept of limit at infinity instead of the fractional derivative used in the RPST. Operating the inverse LT on the obtained Laurent series gives the series solution to the original equation.

The RPST and LRPST present a solution to the DE in a series form. Therefore, the result is supposed to be identical in both methods. But what distinguishes the LRPST from the RPST is the ease of obtaining the series coefficients. The RPST requires the calculation of the fractional derivative to the residual function in each step of determining the coefficients steps. In contrast, the LRPST needs to calculate the limit at infinity when specifying the coefficients. The Caputo derivative is one of the non-local derivatives that need improper integration calculation, and it takes a long time as we progress in the steps of the solution, even when using computer software. Calculating the limit at infinity is much simpler and does not take much time compared to calculating the improper integrals.

Indeed, for the systems (1) and (2), its exact solution is not known yet, and all the solutions given by the previous methods are approximate solutions whose accuracy varies from one method to another. On the other hand, literature doesn't addresses the LRPST for solving systems of fractional DEs to the extent of our knowledge. Therefore, in this paper, we seek to apply the new approach, LRPST [35,50], in creating an accurate analytical series solution to another class of fractional DEs, the FMPS given in (1) and (2). In addition, we look to show the ease, speed, and efficiency of the proposed method to obtain accurate solutions by comparing it with the previous results obtained by other techniques, such as the

Homotopy analysis method and the RPST.

The rest of the presented study is structured as follows: In Section 2, we offer some basic definitions and theorems related to fractional power series. Section 3 discusses the suggested method to construct a series solution to the FMPS. In Section 4, we offer two applications with numerical simulations of MPEs. We summarize and discuss the obtained results in the final section.

2. Main concepts and theorems

Various definitions of the fractional derivative were pointed out previously, such as Hadamard, Riemann Liouville, Caputo, Atangana-Baleanu, Caputo-Fabrizio, conformable, and Riesz definitions. Caputo's view of the fractional derivative is still the most used among other points of view as it has a physical significance in various models and has diverse theorems concerning the expansion of the functions, which is absent from other definitions. Moreover, there is an agreement that Caputo's definition satisfies the fractional derivative conditions. Consequently, during this work, we are interested in considering Caputo's concept, which is defined as follows [51]:

$$D^{\alpha}\rho(\tau)=\begin{cases}\frac{1}{\Gamma(v-\alpha)}\int_0^{\tau}(\tau-\zeta)^{v-\alpha-1}\rho^{(v)}(\zeta)d\zeta, v-1<\alpha<v, 0\leq\zeta<\tau,\\ \rho^{(v)}(\tau), \alpha=v.\end{cases} \tag{3}$$

Next, we introduce some basic definitions, lemmas and facts essential to constructing the Laplace residual power series solution (LRPSS) for the FMPS.

Some significant properties of the Caputo-fractional derivative are $D^{\alpha}(\kappa)=0$, κ is a constant, and $D_{\tau}^{\alpha}(\tau^{\eta})=\frac{\Gamma(\eta+1)}{\Gamma(\eta+1-\alpha)}\tau^{\eta-\alpha}, \tau\geq 0,\ \eta>-1, v-1<\alpha\leq v,\ v\in\mathbb{N}$. For more details, the reader is advised to refer to [51].

Definition 1. [49] Assume that a function $\rho(\tau)$ is specified for $\tau\geq 0$. The LT of $\rho(\tau)$ is designated and given by:

$$P(s)=\ell[\rho(\tau)]=\int_0^{\infty}e^{-s\tau}\rho(\tau)d\tau. \tag{4}$$

Whereas, the inverse LT of $P(s)$ is encoded and defined as:

$$\rho(\tau)=\ell^{-1}[P(s)]=\int_{\mu-i\infty}^{\mu+i\infty}e^{s\tau}P(s)ds,\ \mu=Re(s). \tag{5}$$

Lemma 1. [30] Let $\rho(\tau)$ be a function of exponential order β and piecewise continuous function on $[0,\infty)$. Then,

i) $\lim_{s\to\infty} s\,P(s)=\rho(0)$,

ii) $\ell[D^{\alpha}\rho(\tau)]=s^{\alpha}P(s)-\sum_{n=0}^{v}s^{\alpha-n-1}\rho^{(n)}(0), v-1<\alpha<v,$

iii) $\ell[D^{k\alpha}\rho(\tau)]=s^{k\alpha}P(s)-\sum_{n=0}^{v}s^{(k-n)\alpha-1}D_{\tau}^{n\alpha}\rho(\tau), 0<\alpha<1,$

where, $P(s)=\ell[\rho(\tau)]$ and $D^{k\alpha}=D^{\alpha}D^{\alpha}\ldots D^{\alpha}$ (k-times).

Theorem 1. [46] Assume that $\rho(\tau)$ can be expressed in fractional power series (FPS) of radius R around $\tau=0$ as:

$$\rho(\tau)=\sum_{n=0}^{\infty}\sigma_n\tau^{n\alpha}, 0<\alpha\leq 1, 0\leq\tau<R. \tag{6}$$

If $D^{n\alpha}\rho(\tau)$ is continuous on $(0,R), n=0,1,2,\cdots$, then the coefficients σ_n's of the above series are provided by

$$\sigma_n=\frac{D^{n\alpha}\rho(0)}{\Gamma(n\alpha+1)}, n=0,1,2,\cdots. \tag{7}$$

The next theorem describes the coefficients of the Laurent series expansion (LSE), which is the best tool for constructing the LRPS of a given fractional DE in the Laplace space.

Theorem 2. [29] Assume that $\rho(\tau)$ can be stated in terms of the FPS, and assume that $D^{n\alpha}\rho(\tau)$ is continuous on $(0,R), n=0,1,2,\cdots$. If $P(s)=\ell[\rho(\tau)]$, then $P(s)$ has the following fractional LSE:

$$P(s)=\sum_{n=0}^{\infty}\frac{D^{n\alpha}\rho(0)}{s^{n\alpha+1}}, \tag{8}$$

where $0<\alpha\leq 1, s>0,$ and $n=0,1,2,\cdots$.

The ensuing theorem provides the essential convergence conditions of the LSE.

Theorem 3.[29] Assume that $P(s)=\ell[\rho(\tau)]$ has a fractional LSE. If $\left|s\ell[D^{(n+1)\alpha}\rho(\tau)\right|\leq\gamma$, on $0<s\leq\beta$ where $0<\alpha\leq 1$, and $n\in\mathbb{N}$, then the remainder of the fractional LSE ($\Re_n(s)$) satisfies

$$|\Re_n(s)|\leq\frac{\gamma}{s^{(n+1)\alpha+1}}, 0<s\leq\beta. \tag{9}$$

3. Construction of the LRPSS for the FMPS

This section introduces the LRPST to construct a series solution to the FMPS. We present the method as a seven-step algorithm. Each step includes mathematical procedures and the facts that explain the process.

Step 1. Operate the LT on each equation in (1) and use part (ii) of Lemma 1 to get

$$s^{\alpha}P_r(s)-s^{\alpha-1}\rho_r(0)=\sigma_r P_r(s)+\ell\left[\varphi_r\left(s,\ell^{-1}\left[P_i(s)\right],\frac{1}{\gamma_j}\ell^{-1}\left[P_j\left(\frac{s}{\gamma_j}\right)\right]\right)\right], \tag{10}$$

for $i,j\in\{1,2,\dots,m\}$, and $r=1,2,\dots,m$.

Step 2. Use the conditions (2) with some simplification to rewrite (10) as follows:

$$P_r(s)=\frac{\omega_r}{s}+\frac{\sigma_r}{s^{\alpha}}P_r(s)+\frac{1}{s^{\alpha}}\ell\left[\varphi_r\left(s,\ell^{-1}\left[P_i(s)\right],\frac{1}{\gamma_j}\ell^{-1}\left[P_j\left(\frac{s}{\gamma_j}\right)\right]\right)\right], \tag{11}$$

Step 3. Assume that the LRPSS of (1) and (2) have the following LSE:

$$P_r(s)=\frac{\omega_r}{s}+\sum_{n=1}^{\infty}\frac{h_{r,n}}{s^{n\alpha+1}},\ \ s>0,\ \ r=1,\dots,m. \tag{12}$$

So, the kth truncated series of $P_r(s)$ will be as follows:

$$P_{r,k}(s)=\frac{\omega_r}{s}+\sum_{n=1}^{k}\frac{h_{r,n}}{s^{n\alpha+1}},\ \ s>0,\ \ r=1,\dots,m. \tag{13}$$

Step 4. For every $r=1,2,\dots,m,$ define the Laplace residual functions of (11) as:

$$\ell Res_r(s)=P_r(s)-\frac{\omega_r}{s}-\frac{\sigma_r}{s^{\alpha}}P_r(s)-\frac{1}{s^{\alpha}}\ell\left[\varphi_r\left(s,\ell^{-1}\left[P_i(s)\right],\frac{1}{\gamma_j}\ell^{-1}\left[P_j\left(\frac{s}{\gamma_j}\right)\right]\right)\right], \tag{14}$$

and the kth Laplace residual functions as:

$$\ell Res_{r,k}(s)=P_{r,k}(s)-\frac{\omega_r}{s}-\frac{\sigma_r}{s^{\alpha}}P_{r,k}(s)-\frac{1}{s^{\alpha}}\ell\left[\varphi_r\left(s,\ell^{-1}\left[P_{i,k}(s)\right],\frac{1}{\gamma_j}\ell^{-1}\left[P_{j,k}\left(\frac{s}{\gamma_j}\right)\right]\right)\right]. \tag{15}$$

In this regard, the following facts related to the Laplace residual functions and the kth Laplace residual functions must be mentioned, which are considered basic tools in determining the coefficients of the LSE in (12) [30]:

- $\lim_{k\to\infty}\ell Res_{r,k}(s)=\ell Res_r(s)$, for $s>0,\ r=1,2,\cdots,m$.

- $\ell Res_r(s) = 0$, for $s > 0$, $r = 1,2,\cdots,m$.
- $\lim_{s\to\infty} s^{k\alpha+1}\,\ell Res_r(s) = 0$, for $\alpha, s > 0$, $r = 1,2,\cdots,m$, $k = 0,1,2,\cdots$. (16)
- $\lim_{s\to\infty} s^{k\alpha+1}\,\ell Res_{r,k}(s) = 0$, for $\alpha, s > 0$, $r = 1,2,\cdots,m$, $k = 0,1,2,\cdots$.

Step 5. To determine the value of the coefficient $h_{r,k}$ in the LSE (12) for $r = 1,2,\dots,m$ and $k = 1,2,\dots$, substitute the kth truncated series, $P_{r,k}(s)$, into the kth Laplace residual functions, $\ell Res_{r,n}(s)$ to obtain

$$\ell Res_{r,k}(s) = \sum_{n=1}^{k}\frac{h_{r,n}}{s^{n\alpha+1}} - \frac{\sigma_r}{s^\alpha}P_{r,k}(s) - \frac{1}{s^\alpha}\ell\left[\varphi_r\left(s, \ell^{-1}\left[\frac{\omega_i}{s} + \sum_{n=1}^{k}\frac{h_{i,n}}{s^{n\alpha+1}}\right], \frac{1}{\gamma_j}\ell^{-1}\left[\frac{\gamma_j\omega_j}{s} + \sum_{n=1}^{k}\frac{h_{j,n}(\gamma_j)^{n\alpha+1}}{s^{n\alpha+1}}\right]\right)\right]. \tag{17}$$

Step 6. Substitute (17) into fact (16) and solve the result equation iteratively for $k = 1,2,\dots$ and $r = 1,2,\dots,m$. The solution of resultant equations gives the values of the coefficients of the LSE (12).
Step 7. Substitute the obtained values of the coefficients, $h_{r,k}$, into the kth truncated series (13) and operate the inverse LT on the resultant truncated LSE to obtain the kth approximate LRPSS to the systems (1) and (2).

In the next section, we apply the algorithm described above in detail in two applications. To ensure the accuracy of the obtained results, we use two kinds of errors, the residual error($E^\alpha_{Res_{r,k}}$), and the exact error ($E^\alpha_{Ext_r}$), which are given, respectively, as follows:

$$E^\alpha_{Res_{r,k}} = \left|D^\alpha\rho_{r,k}(\tau) - \sigma_r\rho_{r,k}(\tau) - \varphi_k\left(\tau, \rho_{i,m}(\tau), \rho_{j,m}(\gamma_j\tau)\right)\right|, r = 1,2,\dots,m, k = 1,2,\dots. \tag{18}$$

$$E^\alpha_{Ext_r} = \left|\rho_r(\tau) - \rho_{r,k}(\tau)\right|,\ \ r = 1,2,\dots,m. \tag{19}$$

4. Numerical applications

In this section, we test the proposed method through two applications. The first is a nonhomogeneous FMPS, and the second is a homogeneous FMPS.
Application 4.1. [35] Consider the following nonhomogeneous FMPS:

$$D^\alpha\rho_1(\tau) - \rho_1(\tau) + \rho_2(\tau) - \rho_1\left(\frac{\tau}{2}\right) = e^{-\tau^\alpha} - e^{\frac{\tau^\alpha}{2}},$$

$$D^\alpha\rho_2(\tau) + \rho_1(\tau) + \rho_2(\tau) + \rho_2\left(\frac{\tau}{2}\right) = e^{\frac{-\tau^\alpha}{2}} + e^{\tau^\alpha}, \tag{20}$$

subject to

$$\rho_1(0) = 1,\ \rho_2(0) = 1. \tag{21}$$

Solution: To get the solution of (20) and (21) by LRPST, we first expand the exponential functions in (20) using the expansion of the standard exponential function

$$e^x = 1 + \frac{x}{1!} + \frac{x^2}{2!} + \frac{x^3}{3!} + \cdots.$$

Thus, Eq (20) becomes

$$D^{\alpha}\rho_1(\tau)-\rho_1(\tau)+\rho_2(\tau)-\rho_1\left(\frac{\tau}{2}\right)+\left(\frac{3\tau^{\alpha}}{2}-\frac{3\tau^{2\alpha}}{8}+\frac{3\tau^{3\alpha}}{16}-\frac{5\tau^{4\alpha}}{128}+\frac{11\tau^{5\alpha}}{1280}-\frac{7\tau^{6\alpha}}{5120}\right)=0,$$

$$D^{\alpha}\rho_2(\tau)+\rho_1(\tau)+\rho_2(\tau)+\rho_2\left(\frac{\tau}{2}\right)-\left(2+\frac{\tau^{\alpha}}{2}+\frac{5\tau^{2\alpha}}{8}+\frac{7\tau^{3\alpha}}{48}+\frac{17\tau^{4\alpha}}{384}+\frac{31\tau^{5\alpha}}{3840}+\frac{13\tau^{6\alpha}}{9216}\right)=0. \quad (22)$$

Now, applying LT to each equation in (22) and using the condition (21), we obtain

$$P_1(s)-\frac{1}{s}-\frac{P_1(s)}{s^{\alpha}}+\frac{P_2(s)}{s^{\alpha}}-\frac{2P_1(2s)}{s^{\alpha}}+\frac{1}{s^{\alpha}}\left(\frac{3\Gamma(\alpha+1)}{2\,s^{\alpha+1}}-\frac{3\Gamma(2\alpha+1)}{8\,s^{2\alpha+1}}\right.$$
$$\left.+\frac{3\Gamma(3\alpha+1)}{16\,s^{3\alpha+1}}-\frac{5\Gamma(4\alpha+1)}{128\,s^{4\alpha+1}}+\frac{11\Gamma(5\alpha+1)}{1280\,s^{5\alpha+1}}-\frac{7\Gamma(6\alpha+1)}{5120\,s^{6\alpha+1}}\right)=0,$$

$$P_2(s)-\frac{1}{s}+\frac{P_1(s)}{s^{\alpha}}+\frac{P_2(s)}{s^{\alpha}}+\frac{2P_2(2s)}{s^{\alpha}}-\frac{1}{s^{\alpha}}\left(\frac{2}{s}+\frac{\Gamma(\alpha+1)}{2s^{\alpha+1}}+\frac{5\Gamma(2\alpha+1)}{8\,s^{2\alpha+1}}+\frac{7\Gamma(3\alpha+1)}{48\,s^{3\alpha+1}}+\frac{17\Gamma(4\alpha+1)}{384\,s^{4\alpha+1}}+\frac{31\Gamma(5\alpha+1)}{3840\,s^{5\alpha+1}}+\right.$$
$$\left.\frac{13\Gamma(6\alpha+1)}{9216\,s^{6\alpha+1}}\right)=0. \quad (23)$$

According to the previous section, the kth truncated series of the supposed series solution of the systems (20) and (21) is given as:

$$P_{1,k}(s)=\frac{1}{s}+\sum_{n=1}^{k}\frac{h_{1,n}}{s^{n\alpha+1}},\ P_{2,k}(s)=\frac{1}{s}+\sum_{n=1}^{k}\frac{h_{2,n}}{s^{n\alpha+1}}. \quad (24)$$

Consequently, the kth Laplace residual functions of (23) can be defined as:

$$\ell Res_{1,k}(s)=\ P_{1,k}(s)-\frac{1}{s}-\frac{P_{1,k}(s)}{s^{\alpha}}+\frac{P_{2,k}(s)}{s^{\alpha}}-\frac{2P_{1,k}(2s)}{s^{\alpha}}$$
$$+\frac{1}{s^{\alpha}}\left(\frac{3\Gamma(\alpha+1)}{2\,s^{\alpha+1}}-\frac{3\Gamma(2\alpha+1)}{8\,s^{2\alpha+1}}+\frac{3\Gamma(3\alpha+1)}{16\,s^{3\alpha+1}}\right.$$
$$\left.-\frac{5\Gamma(4\alpha+1)}{128\,s^{4\alpha+1}}+\frac{11\Gamma(5\alpha+1)}{1280\,s^{5\alpha+1}}-\frac{7\Gamma(6\alpha+1)}{5120\,s^{6\alpha+1}}\right),$$

$$\ell Res_{2,k}(s)=\ P_{2,k}(s)-\frac{1}{s}+\frac{P_{1,k}(s)}{s^{\alpha}}+\frac{P_{2,k}(s)}{s^{\alpha}}+\frac{2P_{2,k}(2s)}{s^{\alpha}}-\frac{1}{s^{\alpha}}\left(\frac{2}{s}+\frac{\Gamma(\alpha+1)}{2s^{\alpha+1}}+\frac{5\Gamma(2\alpha+1)}{8\,s^{2\alpha+1}}+\frac{7\Gamma(3\alpha+1)}{48\,s^{3\alpha+1}}+\right.$$
$$\left.\frac{17\Gamma(4\alpha+1)}{384\,s^{4\alpha+1}}+\frac{31\Gamma(5\alpha+1)}{3840\,s^{5\alpha+1}}+\frac{13\Gamma(6\alpha+1)}{9216\,s^{6\alpha+1}}\right). \quad (25)$$

By substituting $k=1$ in (25), the first Laplace residual function will be as:

$$\ell Res_{1,1}(s)=\frac{h_{1,1}}{s^{\alpha+1}}-\frac{h_{1,1}}{s^{2\alpha+1}}+\frac{h_{2,1}}{s^{2\alpha+1}}-\frac{1}{s^{\alpha+1}}-\frac{h_{1,1}}{2^{\alpha}s^{2\alpha+1}}+\frac{3\Gamma(\alpha+1)}{2\,s^{2\alpha+1}}-\frac{3\Gamma(2\alpha+1)}{8\,s^{3\alpha+1}}$$
$$+\frac{3\Gamma(1+3\alpha)}{16\,s^{4\alpha+1}}-\frac{5\Gamma(1+4\alpha)}{128\,s^{5\alpha+1}}+\frac{11\Gamma(1+5\alpha)}{1280\,s^{6\alpha+1}}-\frac{7\Gamma(1+6\alpha)}{5120\,s^{7\alpha+1}},$$

$$\ell Res_{2,1}(s)=\frac{h_{2,1}}{s^{\alpha+1}}+\frac{h_{1,1}}{s^{2\alpha+1}}+\frac{h_{2,1}}{s^{2\alpha+1}}+\frac{1}{s^{\alpha+1}}+\frac{h_{2,1}}{2^{\alpha}s^{2\alpha+1}}-\frac{\Gamma(\alpha+1)}{2s^{2\alpha+1}}-\frac{5\Gamma(2\alpha+1)}{8\,s^{3\alpha+1}}-\frac{7\Gamma(1+3\alpha)}{48\,s^{4\alpha+1}}-\frac{17\Gamma(1+4\alpha)}{384\,s^{5\alpha+1}}-\frac{31\Gamma(5\alpha+1)}{3840\,s^{6\alpha+1}}-\frac{13\Gamma(6\alpha+1)}{9216\,s^{7\alpha+1}}. \tag{26}$$

By multiplying each equation in (26) by $s^{\alpha+1}$, we get the following new system:

$$s^{\alpha+1}\ell Res_{1,1}(s)=h_{1,1}-1-\frac{h_{1,1}}{s^{\alpha}}+\frac{h_{2,1}}{s^{\alpha}}-\frac{h_{1,1}}{2^{\alpha}s^{\alpha}}+\frac{3\Gamma(\alpha+1)}{2\,s^{\alpha}}-\frac{3\Gamma(2\alpha+1)}{8\,s^{2\alpha}}+\frac{3\Gamma(3\alpha+1)}{16\,s^{3\alpha}}-\frac{5\Gamma(4\alpha+1)}{128\,s^{4\alpha}}+\frac{11\Gamma(5\alpha+1)}{1280\,s^{5\alpha}}-\frac{7\Gamma(6\alpha+1)}{5120\,s^{6\alpha}},$$

$$s^{\alpha+1}\ell Res_{2,1}(s)=h_{2,1}+1+\frac{h_{1,1}}{s^{\alpha}}+\frac{h_{2,1}}{s^{\alpha}}+\frac{h_{2,1}}{2^{\alpha}s^{\alpha}}-\frac{\Gamma(\alpha+1)}{2s^{\alpha}}-\frac{5\Gamma(2\alpha+1)}{8\,s^{2\alpha}}-\frac{7\Gamma(3\alpha+1)}{48\,s^{3\alpha}}-\frac{17\Gamma(4\alpha+1)}{384\,s^{4\alpha}}-\frac{31\Gamma(5\alpha+1)}{3840\,s^{5\alpha}}-\frac{13\Gamma(6\alpha+1)}{9216\,s^{6\alpha}}. \tag{27}$$

Taking the limit as s goes to infinity in (27) gives $h_{1,1}=1$ and $h_{2,1}=-1$.
By repeating the previous procedure for $k=2,3,4,5,$ and 6, we can simply obtain the following coefficients:

$$h_{1,2}=\left(2+\frac{1}{2^{\alpha}}-\frac{3\Gamma(\alpha+1)}{2}\right)\text{ and }\ h_{2,2}=\left(\frac{1}{2^{\alpha}}+\frac{\Gamma(\alpha+1)}{2}\right). \tag{28}$$

$$h_{1,3}=\frac{1}{8^{\alpha+1}}\left(8+2^{\alpha+4}+2^{3\alpha+4}-2^{\alpha+2}(3+4^{\alpha+1})\Gamma(\alpha+1)+3(2)^{3\alpha}\Gamma(1+2\alpha)\right),$$

$$h_{2,3}=-2-2^{1-\alpha}-2^{-3\alpha}+(1-2^{-2\alpha-1})\Gamma(\alpha+1)+\frac{5}{8}\Gamma(2\alpha+1), \tag{29}$$

...

$$\begin{aligned}h_{1,6}=\Bigg(&8+2^{1-14\alpha}+2^{1-11\alpha}+32^{1-10\alpha}+2^{2-9\alpha}+52^{1-7\alpha}+2^{1-6\alpha}+3\,(2)^{2-5\alpha}+2^{2-\alpha}+2^{-15\alpha}\\&+4^{1-6\alpha}+4^{1-4\alpha}+4^{1-2\alpha}+4^{1-\alpha}+8^{1-\alpha}-\frac{1}{2}\Gamma(1+2\alpha)\\&-2^{-4-9\alpha}\left(9+2^{1+5\alpha}+9(2)^{1+9\alpha}+\frac{16^{1+\alpha}}{3}\right)\Gamma(1+3\alpha)+6\Gamma(1+\alpha)\\&-32^{-1-14\alpha}\Gamma(1+\alpha)-2^{1-12\alpha}\Gamma(1+\alpha)-2^{1-10\alpha}\Gamma(1+\alpha)-2^{2-9\alpha}\Gamma(1+\alpha)\\&-32^{1-7\alpha}\Gamma(1+\alpha)-2^{1-4\alpha}\Gamma(1+\alpha)-2^{2-3\alpha}\Gamma(1+\alpha)-2^{1-2\alpha}\Gamma(1+\alpha)\\&-2^{-11\alpha}\Gamma(1+\alpha)-2^{-8\alpha}\Gamma(1+\alpha)+2^{-6\alpha}\Gamma(1+\alpha)-72^{-5\alpha}\Gamma(1+\alpha)\\&-2^{-2-9\alpha}\,\Gamma(1+2\alpha)-2^{-2-7\alpha}\,\Gamma(1+2\alpha)+3\,(2)^{-2-5\alpha}\Gamma(1+2\alpha)\\&+\ 32^{-2-5\alpha}\Gamma(1+2\alpha)+2^{-8\alpha}\Gamma(1+2\alpha)-54^{-1-2\alpha}\Gamma(1+2\alpha)+38^{-1-4\alpha}\Gamma(1+2\alpha)\\&-\frac{1}{192}\Gamma(1+4\alpha)+52^{-7-5\alpha}\Gamma(1+4\alpha)-\frac{11\Gamma(1+5\alpha)}{1280}\Bigg),\end{aligned}$$

$$h_{2,6} = \Big(\frac{2^{-8-15\alpha}}{15}(3840 + 152^{9+2\alpha} + (15)2^{11+7\alpha} - (15)2^{9+8\alpha} - (15)2^{10+13\alpha} + (15)4^{5+6\alpha}$$
$$+ (15)4^{5+7\alpha} + (15)8^{3+\alpha} + (15)32^{2+\alpha} + (15)512^{1+\alpha} + (15)1024^{1+\alpha}$$
$$+ (15)2^{7+\alpha}(1 - 2^{1+2\alpha} + 2^{2+3\alpha} - 2^{1+4\alpha} + 32^{1+5\alpha} - (3)2^{1+6\alpha} + 2^{2+7\alpha} + (3)2^{1+8\alpha}$$
$$- 2^{1+9\alpha} + 2^{3+10\alpha} - 2^{2+11\alpha} + 4^{1+7\alpha} + 8^{1+4\alpha})\Gamma(1+\alpha)$$
$$- (15)8^{2+\alpha}(5 + 2^{1+4\alpha} + 52^{1+7\alpha} + 2^{1+9\alpha})\alpha\Gamma(2\alpha) + 152^{8+11\alpha}\alpha\Gamma(3\alpha)$$
$$+ 1054^{2+3\alpha}\alpha\Gamma(3\alpha) - (15)32^{1+2\alpha}\alpha\Gamma(3\alpha) - 452^{6+11\alpha}\Gamma(1+2\alpha)$$
$$- 154^{4+3\alpha}\Gamma(1+2\alpha) - (15)8^{3+5\alpha}\Gamma(1+2\alpha) - (15)16^{2+3\alpha}\Gamma(1+2\alpha)$$
$$- 15256^{1+\alpha}\Gamma(1+2\alpha) + (35)32^{1+3\alpha}\Gamma(1+3\alpha) - 852^{1+10\alpha}\Gamma(1+4\alpha)$$
$$- 58^{2+5\alpha}\Gamma(1+4\alpha) + 312^{15\alpha}\Gamma(1+5\alpha)\Big).$$

Therefore, the fractional Laurent series solution of (23) can be expressed as

$$P_1(s) = \frac{1}{s} + \frac{1}{s^{\alpha+1}} + \left(2 + \frac{1}{2^{\alpha}} - \frac{3\Gamma(\alpha+1)}{2}\right)\frac{1}{s^{2\alpha+1}}$$
$$+ \frac{1}{8^{\alpha+1}s^{3\alpha+1}}\left(8 + 2^{\alpha+4} + 2^{3\alpha+4} - 2^{\alpha+2}(3 + 4^{\alpha+1})\Gamma(\alpha+1) + 38^{\alpha}\Gamma(1+2\alpha)\right)$$
$$+ \cdots,$$

$$P_2(s) = \frac{1}{s} - \frac{1}{s^{\alpha+1}} + \left(\frac{1}{2^{\alpha}} + \frac{\Gamma(\alpha+1)}{2}\right)\frac{1}{s^{2\alpha+1}} + \frac{1}{s^{3\alpha+1}}\Big(-2 - 2^{1-\alpha} - 2^{-3\alpha} + (1 - 2^{-2\alpha-1})\Gamma(1+\alpha) + \frac{5}{8}\Gamma(1+2\alpha)\Big) + \cdots. \tag{30}$$

To obtain the series solution to the systems (20) and (21), we apply the inverse LT to (30), and then we get

$$\rho_1(\tau) = 1 + \left(2 + \frac{1}{2^{\alpha}} - \frac{3\Gamma(\alpha+1)}{2}\right)\frac{\tau^{\alpha}}{\Gamma(\alpha+1)}$$
$$+ \frac{1}{8^{\alpha+1}}\Big(8 + 2^{\alpha+4} + 2^{3\alpha+4} - 2^{\alpha+2}(3 + 4^{\alpha+1})\Gamma(\alpha+1)$$
$$+ 3(2)^{3\alpha}\Gamma(2\alpha+1)\Big)\frac{\tau^{2\alpha}}{\Gamma(2\alpha+1)} + \cdots,$$

$$\rho_2(\tau) = 1 + \left(\frac{1}{2^{\alpha}} + \frac{\Gamma(\alpha+1)}{2}\right)\frac{\tau^{\alpha}}{\Gamma(\alpha+1)} - \left(2 + \frac{1}{2^{\alpha-1}} + \frac{1}{2^{3\alpha}} - \left(1 - \frac{1}{2^{2\alpha+1}}\right)\Gamma(\alpha+1) - \frac{5}{8}\Gamma(2\alpha+1)\right)\frac{\tau^{2\alpha}}{\Gamma(2\alpha+1)} + \cdots. \tag{31}$$

Putting $\alpha = 1$ in (31) gives the solution of (20) and (21) in the following form:

$$\rho_1(\tau) = 1 + \tau + \frac{\tau^2}{2} + \frac{\tau^3}{8} + \cdots,$$

$$\rho_2(\tau) = 1 - \tau + \frac{\tau^2}{2} - \frac{\tau^3}{8} + \cdots,$$

which are the expansions of the exact solutions $\rho_1(\tau) = e^{\tau}$, $\rho_2(\tau) = e^{-\tau}$.

To verify the accuracy of the solution obtained in Eq (31) and to clarify the effect of changing α value on the behavior of the solution, some illustrations have been drawn in Figures 1–4. Figures 1(a) and 2(a). show comparisons between the 6th approximate solution given in (31) and the exact solution of the systems (20) and (21) at $\alpha = 1$. The results indicate a great agreement between the two solutions in the period $[0,3]$.

Figures 1(b) and 2(b) show the behavior of the systems (20) and (21) solution with different values of α, which are 0.5, 0.7 and 1. It can be seen from the figure that as the value of α changes, the level of motion represented by the dependent variables in FMPS changes more or less.

Since we have the exact solution for the systems (20) and (21) at $\alpha = 1$, we introduce in Figure 3 the exact error of the 6th approximation for the solution given in (31) and it appears to be mathematically acceptable.

In Figure 4, we make a comparison between the solution obtained by LRPST and the solution obtained by HAM with the exact solution at $\alpha = 1$. It is evident from the figure that the LRPSS is more compatible with the exact solution than with the HAM solution.

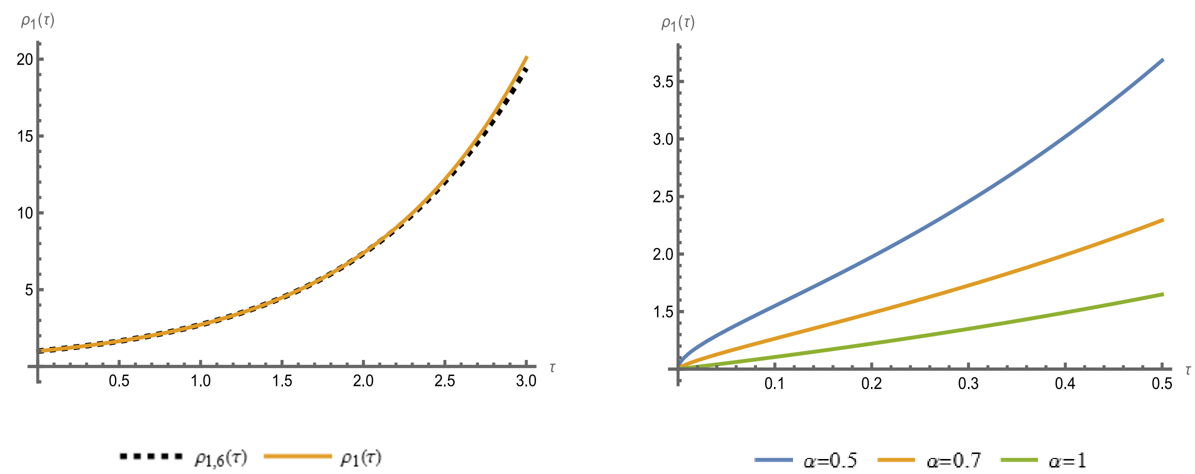

(a) (b)

Figure 1. The graph of (a) the exact solution, $\rho_1(\tau) = e^{\tau}$ and the 6th approximate solution, $\rho_{1,6}(\tau)$ at $\alpha = 1$, (b) $\rho_{1,6}(\tau)$ at $\alpha = 1, 0.7, 0.5$.

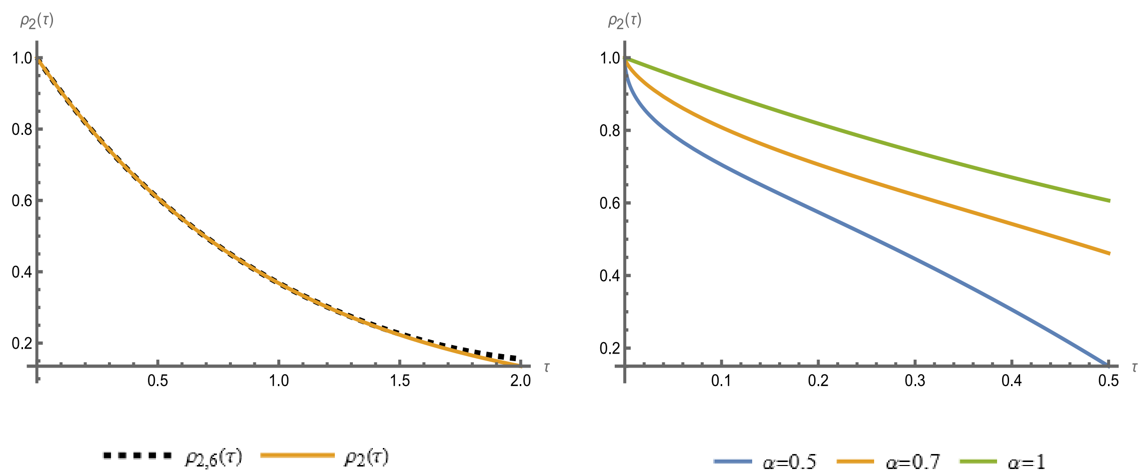

(a) (b)

Figure 2. The graph of (a) the exact solution, $\rho_2(\tau) = e^{-\tau}$ and the 6th approximate solution, $\rho_{2,6}(\tau)$ at $\alpha = 1$, (b) $\rho_{2,6}(\tau)$ at $\alpha = 1, 0.7, 0.5$.

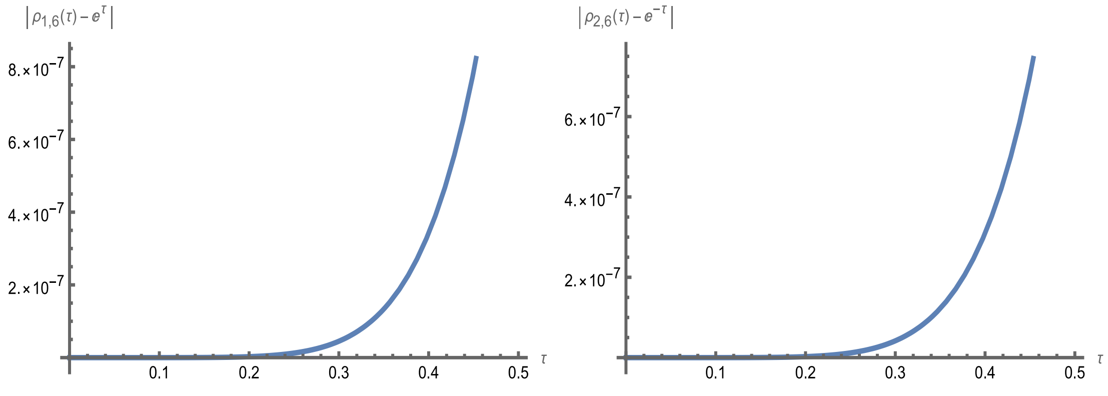

(a) (b)

Figure 3. The exact error of (a) the 6th approximate solution, $\rho_{1,6}(\tau)$ (b) the 6th approximate solution, $\rho_{2,6}(\tau)$ at $\alpha = 1$.

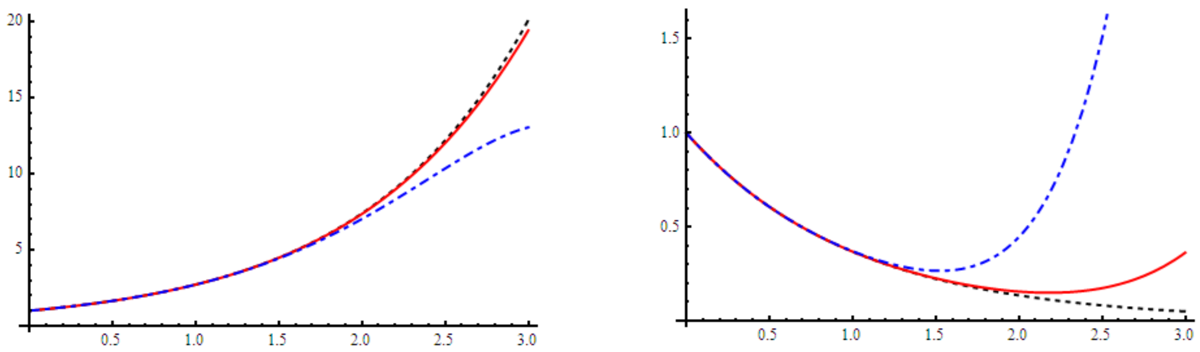

(a) (b)

Figure 4. The graphs of the 6th approximate solution of the systems (20) and (21) when $\alpha = 1$: Dotted Line: LRPST solution, Dashed Dotted Line: HAM ($\hbar = -1$) solution, Solid Line: Exact solution. (a) $\rho_{1,6}(\tau)$, (b) $\rho_{2,6}(\tau)$.

For further analysis of the solution that we obtained in Application 4.1, we consider two types of errors, the exact errors, $E^{\alpha}_{\mathrm{Ext}_1}$ and $E^{\alpha}_{\mathrm{Ext}_2}$, and the residual errors, $E^{\alpha}_{Res_1}$ and $E^{\alpha}_{Res_2}$ of the approximate solution in (31) which are defined, respectively, as:

$$E^{\alpha}_{\mathrm{Ext}_1} = \left|\rho_1(\tau) - \rho_{1,k}(\tau)\right|,$$

$$E^{\alpha}_{\mathrm{Ext}_2} = \left|\rho_2(\tau) - \rho_{2,k}(\tau)\right|,$$

$$E^{\alpha}_{\ell Res_1} = \left|D^{\alpha}\rho_{1,k}(\tau) - \rho_{1,k}(\tau) + \rho_{2,k}(\tau) - \rho_{1,k}\left(\frac{\tau}{2}\right) - \mathrm{e}^{-\tau} + \mathrm{e}^{\tau/2}\right|,$$

$$E^{\alpha}_{\ell Res_2} = \left|D^{\alpha}\rho_{2,k}(\tau) + \rho_{1,k}(\tau) + \rho_{2,k}(\tau) + \rho_{2,k}\left(\frac{\tau}{2}\right) - \mathrm{e}^{\tau} - \mathrm{e}^{-\tau/2}\right|.$$

Tables 1 and 2 confirm numerically the accuracy of the solution we obtained by calculating the exact and residual errors of the approximate solution in (31) at $\alpha = 1$ and 0.5. In addition, they present comparisons between the new solution and the previous solutions obtained by the RPST and HAM methods. The tables show the agreement between the results obtained from LRPST and RPST, which proves the proposed method's efficiency and that LRPST is much easier and faster to program and performs calculations. Moreover, we can see from the tables that LRPST is better than HAM: the solution obtained from LRPST converges faster to the exact solution, and the error is slightly smaller than the errors obtained using HAM.

Table 1. The exact, $E_{Ext_1}^{\alpha=1}(\tau)$ and the residual, $E_{Res_1}^{\alpha=0.5}(\tau)$ errors of $\rho_{1,6}(\tau)$.

	$E_{Ext_1}^{\alpha=1}(\tau)$			$E_{Res_1}^{\alpha=0.5}(\tau)$		
t	LRPST	HAM ($\hbar = -1$)	RPST	LRPST	HAM ($\hbar = -1$)	RPST
0.0	0	0	0	0	0	0
0.2	2.60461×10^{-9}	2.91038×10^{-8}	2.60461×10^{-9}	8.88889×10^{-8}	9.66713×10^{-7}	8.88889×10^{-8}
0.4	3.42086×10^{-7}	3.85358×10^{-6}	3.42086×10^{-7}	5.68889×10^{-6}	5.94783×10^{-5}	5.68889×10^{-6}
0.6	6.00039×10^{-6}	6.75053×10^{-5}	6.00039×10^{-6}	6.47999×10^{-5}	6.51337×10^{-4}	6.47999×10^{-5}
0.8	4.61729×10^{-5}	5.18636×10^{-4}	4.61729×10^{-5}	3.64089×10^{-4}	3.51558×10^{-3}	3.64089×10^{-4}
1.0	2.26273×10^{-4}	253712×10^{-3}	2.26273×10^{-4}	1.38889×10^{-3}	1.28713×10^{-2}	1.38889×10^{-3}

Table 2. The exact, $E_{Ext_2}^{\alpha=1}(\tau)$ and the residual, $E_{Res_2}^{\alpha=0.5}(\tau)$ errors of $\rho_{2,6}(\tau)$.

	$E_{Ext_2}^{\alpha=1}(\tau)$			$E_{Res_2}^{\alpha=0.5}(\tau)$		
t	LRPST	HAM ($\hbar = -1$)	RPST	LRPST	HAM ($\hbar = -1$)	RPST
0.0	0	0	0	0	0	0
0.2	2.47757×10^{-9}	3.62052×10^{-8}	2.47757×10^{-9}	8.88889×10^{-8}	1.27079×10^{-6}	8.88889×10^{-8}
0.4	3.09519×10^{-7}	4.55603×10^{-6}	3.09519×10^{-7}	5.68889×10^{-6}	8.01156×10^{-5}	5.68889×10^{-6}
0.6	5.16391×10^{-6}	7.66634×10^{-5}	5.16391×10^{-6}	6.47999×10^{-5}	8.98412×10^{-4}	6.47999×10^{-5}
0.8	3.77914×10^{-5}	5.65864×10^{-4}	3.77914×10^{-5}	3.64089×10^{-4}	4.96166×10^{-3}	3.64089×10^{-4}
1.0	1.76114×10^{-4}	2.65956×10^{-3}	1.76114×10^{-4}	1.38889×10^{-3}	1.85716×10^{-2}	1.38889×10^{-3}

Application 4.2. [35] Consider the following homogeneous FMPS:

$$D^{\alpha}\rho_1(\tau) + \rho_1(\tau) + e^{-\tau^{\alpha}}\cos\left(\frac{\tau^{\alpha}}{2}\right)\rho_2\left(\frac{\tau}{2}\right) + 2e^{-\frac{3\tau^{\alpha}}{4}}\cos\left(\frac{\tau^{\alpha}}{2}\right)\sin\left(\frac{\tau^{\alpha}}{4}\right)\rho_1\left(\frac{\tau}{4}\right) = 0,$$

$$D^{\alpha}\rho_2(\tau) - e^{\tau^{\alpha}}\rho_1^2\left(\frac{\tau}{2}\right) + \rho_2^2\left(\frac{\tau}{2}\right) = 0, \tag{32}$$

subject to

$$\rho_1(0) = 1,\ \rho_2(0) = 0, \tag{33}$$

which has an exact solution in the case of $\alpha = 1$ as follows:

$$\rho_1(\tau) = e^{-\tau}\cos\tau, \rho_2(\tau) = \sin\tau.$$

Solution: As in the previous application, apply LT to every equation in (32) to get

$$P_1(s)-\frac{1}{s}+\frac{P_1(s)}{s^\alpha}+\frac{1}{s^\alpha}\ell\left[e^{-\tau^\alpha}\cos\left(\frac{\tau^\alpha}{2}\right)2\,\ell^{-1}[P_2(2s)]\right]$$

$$+\frac{1}{s^\alpha}\ell\left[2e^{-\frac{3\tau^\alpha}{4}}\cos\left(\frac{\tau^\alpha}{2}\right)\sin\left(\frac{\tau^\alpha}{4}\right)4\,\ell^{-1}[P_1(4s)]\right]=0,$$

$$P_2(s)-\frac{1}{s^\alpha}\ell\left[e^{\tau^\alpha}(\ell^{-1}[2P_1(2s)])^2\right]+\frac{1}{s^\alpha}\ell[(\ell^{-1}[2P_2(2s)])^2]=0. \quad (34)$$

Depending on our approach taken in Section 3, assume that the kth approximate series solutions of (34) have the following expansions:

$$P_{1,k}(s)=\frac{1}{s}+\sum_{n=1}^{k}\frac{h_{1,n}}{s^{n\alpha+1}},\ P_{2,k}(s)=\frac{1}{s}+\sum_{n=1}^{k}\frac{h_{2,n}}{s^{n\alpha+1}}. \quad (35)$$

Therefore, the kth Laplace residual functions of (34) are as follows:

$$\ell Res_{1,k}(s)=\ P_{1,k}(s)-\frac{1}{s}-\frac{P_{1,k}(s)}{s^\alpha}+\frac{1}{s^\alpha}\ell\left[e^{-\tau^\alpha}\cos\left(\frac{\tau^\alpha}{2}\right)2\,\ell^{-1}\left[P_{2,k}(2s)\right]\right]$$

$$+\frac{1}{s^\alpha}\ell\left[2e^{-\frac{3\tau^\alpha}{4}}\cos\left(\frac{\tau^\alpha}{2}\right)\sin\left(\frac{\tau^\alpha}{4}\right)4\,\ell^{-1}\left[P_{1,k}(4s)\right]\right]=0,$$

$$\ell Res_{2,k}(s)=\ P_{2,k}(s)-\frac{1}{s^\alpha}\ell\left[e^{\tau^\alpha}\left(\ell^{-1}\left[2P_{1,k}(2s)\right]\right)^2\right]+\frac{1}{s^\alpha}\ell\left[\left(\ell^{-1}\left[2P_{2,k}(2s)\right]\right)^2\right]=0. \quad (36)$$

As in the previous example, recursively, we substitute $k=1,2,...$ into (36), multiply each equation in it by $s^{k\alpha+1}$, and then take the limit as $s\to\infty$ to find the coefficients of series solution in (35) as follows:

$h_{1,1}=-1,$

$h_{2,1}=1,$

$h_{1,2}=\left(1-2^{-\alpha}-2^{-1}\Gamma(\alpha+1)\right),$

$h_{2,2}=\left(-2^{1-\alpha}+\Gamma(\alpha+1)\right),$

$$h_{1,3}=\frac{1}{8^{\alpha+1}}\left(-1+2^{1-3\alpha}+2^{-\alpha}+\left(\frac{1}{2}-2^{-2\alpha}\right)\Gamma(1+\alpha)+\frac{(1+2^{1+\alpha})\Gamma\left(\frac{1}{2}+\alpha\right)}{2\sqrt{\pi}}+\frac{3}{8}\Gamma(1+2\alpha)\right),$$

$$h_{2,3}=\frac{1}{2}\Gamma(1+2\alpha)+8^{-\alpha}\left(-2+2^{1+\alpha}-\frac{2^{1+4\alpha}\Gamma\left(\frac{1}{2}+\alpha\right)}{\sqrt{\pi}}-2^{\alpha}\Gamma(1+\alpha)\right),$$

$$h_{1,4}=\Bigg(1+2^{1-6\alpha}-2^{1-5\alpha}-2^{1-3\alpha}-2^{-\alpha}-\frac{1}{2}\Gamma(1+\alpha)-\frac{8^{-\alpha}}{2}\Gamma(1+2\alpha)$$
$$-\frac{2^{-1-2\alpha}}{\sqrt{\pi}}(-4+2^{1+3\alpha}+4^{\alpha})\Gamma\left(\frac{1}{2}+\alpha\right)-\frac{3}{8}\Gamma(1+2\alpha)-\frac{7}{96}\Gamma(1+3\alpha)$$
$$+\frac{4^{-1-3\alpha}\sqrt{\pi}\,\Gamma(1+3\alpha)}{\Gamma\left(\frac{1}{2}+\alpha\right)}-\frac{3(2)^{-3-2\alpha}(1+2\alpha)\Gamma(1+3\alpha)}{\Gamma(1+\alpha)}$$
$$-2^{-1-5\alpha}(-1+2^{\alpha}+4^{1+\alpha})\frac{\Gamma(1+3\alpha)}{\Gamma(1+2\alpha)}$$
$$+\frac{2^{-5\alpha}\Gamma(1+\alpha)\big((1+8^{\alpha})\Gamma(1+2\alpha)+8^{\alpha}\Gamma(1+3\alpha)\big)}{\Gamma(1+2\alpha)}\Bigg),$$

$$h_{2,4}=\Bigg(2^{1-6\alpha}(2+4^{\alpha}-8^{\alpha})-2^{1-5\alpha}\Gamma(1+\alpha)+\frac{8^{-\alpha}(1+2^{1+\alpha})}{\sqrt{\pi}}\Gamma\left(\frac{1}{2}+\alpha\right)-\frac{2^{-\alpha}\Gamma(1+3\alpha)}{\Gamma(1+\alpha)}$$
$$+8^{-\alpha}\Gamma(1+\alpha)+3\,(2)^{-2-3\alpha}\Gamma(1+2\alpha)+\frac{1}{6}\Gamma(1+3\alpha)+\frac{4^{-\alpha}\,\Gamma(1+3\alpha)}{\Gamma^{2}(1+\alpha)}$$
$$-8^{-\alpha}\big(3-2^{1+\alpha}+2^{\alpha}\Gamma(1+\alpha)\big)\frac{\Gamma(1+3\alpha)}{\Gamma(1+2\alpha)}-\frac{2^{1-4\alpha}(-3+2^{\alpha})\Gamma(1+3\alpha)}{\Gamma(1+\alpha)\Gamma(1+2\alpha)}\Bigg).$$

Thus, we can express the 5th approximate series solution of (34) as:

$$P_1(s)=\frac{1}{s}-\frac{1}{s^{\alpha+1}}+\left(1-\frac{1}{2^{\alpha}}-\frac{\Gamma(\alpha+1)}{2}\right)\frac{1}{s^{2\alpha+1}}+\frac{h_{1,3}}{s^{3\alpha+1}}+\frac{h_{1,4}}{s^{4\alpha+1}},$$

$$P_2(s)=\frac{1}{s^{\alpha+1}}-\left(2^{1-\alpha}-\Gamma(\alpha+1)\right)\frac{1}{s^{2\alpha+1}}+\frac{h_{2,3}}{s^{3\alpha+1}}+\frac{h_{2,4}}{s^{4\alpha+1}}. \tag{37}$$

To get the solution of the system (32) and (33) in the original space, we apply the inverse LT to (37) to get

$$\rho_1(\tau)=1-\frac{\tau^{\alpha}}{\Gamma(1+\alpha)}+\left(1-\frac{1}{2^{\alpha}}-\frac{\Gamma(\alpha+1)}{2}\right)\frac{\tau^{2\alpha}}{\Gamma(1+2\alpha)}+\frac{h_{1,3}\tau^{3\alpha}}{\Gamma(1+3\alpha)}+\frac{h_{1,4}\tau^{4\alpha}}{\Gamma(1+4\alpha)},$$

$$\rho_2(\tau)=\frac{\tau^{\alpha}}{\Gamma(1+\alpha)}+\left(-2^{1-\alpha}+\Gamma(1+\alpha)\right)\frac{\tau^{2\alpha}}{\Gamma(1+2\alpha)}+\frac{h_{2,3}\tau^{3\alpha}}{\Gamma(1+3\alpha)}+\frac{h_{2,4}\tau^{4\alpha}}{\Gamma(1+4\alpha)}. \tag{38}$$

We can verify that at $\alpha=1$, the 5th approximate series solution in (38) becomes as follows:

$$\rho_1^6(\tau)=1-\tau+\frac{\tau^3}{3}-\frac{\tau^4}{6}+\frac{\tau^5}{30},$$

$$\rho_2^6(\tau)=\tau-\frac{\tau^3}{6}+\frac{\tau^5}{120}, \tag{39}$$

that coincide with the first six terms of the expansion of the exact solutions.

Likewise, in this application, the solution that we obtained was analyzed to verify its accuracy by reviewing some graphs and numerical tables. Figures 5(a) and 6(a) show the high agreement between the approximate and exact solution when $\alpha = 1$. Figures 5(b) and 6(b) present the solution in (38) at different values of α, which are 0.5, 0.7 and 1. The curves show that the movement of the particle changes by increasing or decreasing according to the change in the value of α. This confirms what we mentioned earlier: The value of α affects the movement. Figure 7 shows the exact error of the fifth approximation for the solution given in (39) and it seems to be very acceptable mathematically in the period shown.

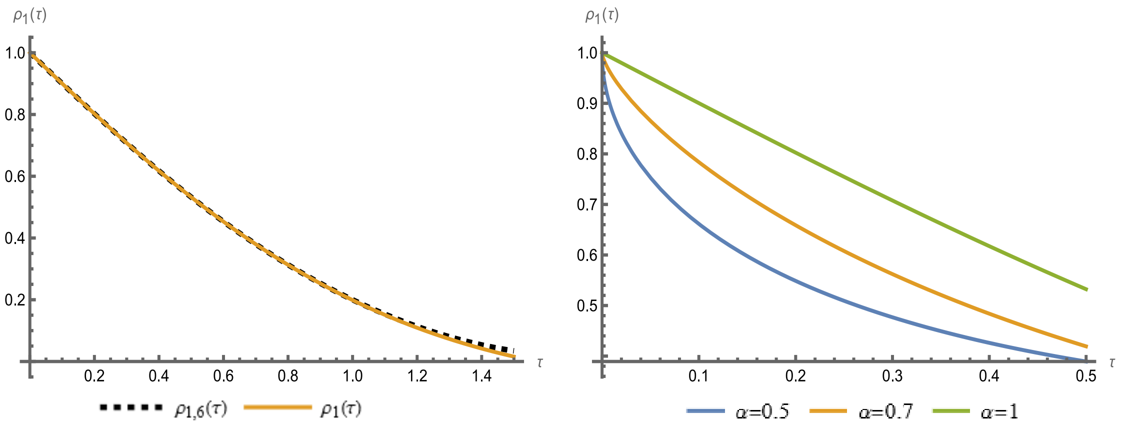

(a) (b)

Figure 5. The graphs of (a) the exact solution, $\rho_1(\tau)$ and the 5th approximate solution, $\rho_{1,5}(\tau)$ at $\alpha = 1$, (b) the 5th approximate solution, $\rho_{1,5}(\tau)$ at different values of α $(\alpha = 1, 0.7, 0.5)$ using the LRPST.

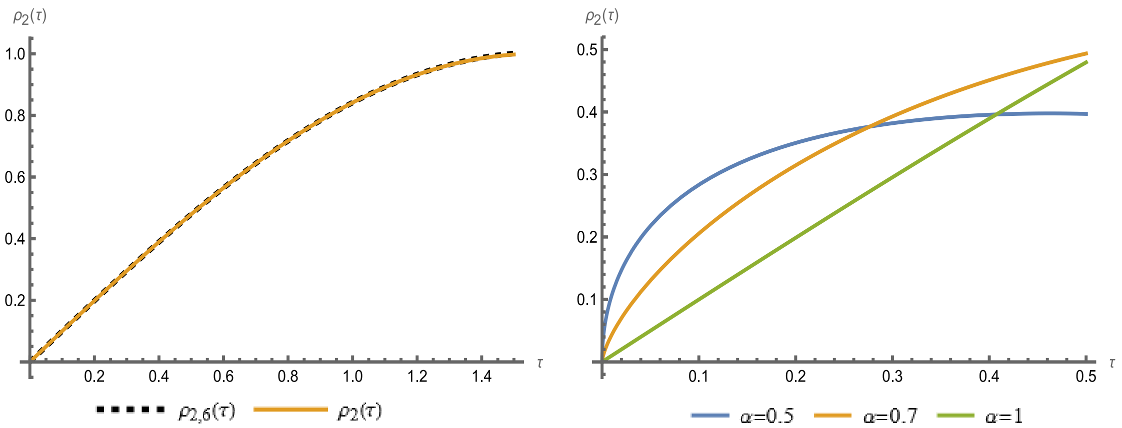

(a) (b)

Figure 6. The graphs of (a) the exact solution, $\rho_2(\tau)$ and the 5th approximate solution, $\rho_{2,5}(\tau)$ at $\alpha = 1$, (b) the 5th approximate solution, $\rho_{2,5}(\tau)$ at different values of α $(\alpha = 1, 0.7, 0.5)$ using the LRPST.

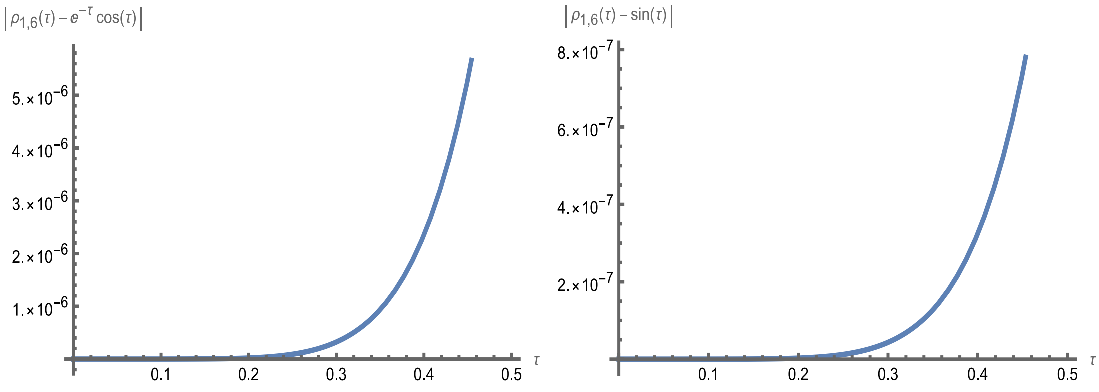

(a) (b)

Figure 7. The exact error of (a) the 5th approximate solution, $\rho_{1,5}(\tau)$, (b) the 5th approximate solution, $\rho_{2,5}(\tau)$ at $\alpha = 1$.

In the following two tables, Tables 3 and 4, we present two types of errors, exact and residual, related to Application 4.2 for the present approximation and previous approximations prepared by the RPST and HAM methods.

Table 3. The exact, $E_{Ext_1}^{\alpha=1}(\tau)$ and the residual, $E_{Res_1}^{\alpha=0.5}(\tau)$ errors of $\rho_{1,6}(\tau)$.

	$E_{Ext_1}^{\alpha=1}(\tau)$			$E_{Res_1}^{\alpha=0.5}(\tau)$		
t	LRPST	HAM($\hbar=-1$)	RPST	LRPST	HAM($\hbar=-1$)	RPST
0.0	0	0	0	0	0	0
0.2	1.93×10^{-8}	6.44×10^{-8}	1.93×10^{-8}	4.40×10^{-4}	3.94×10^{-4}	4.40×10^{-4}
0.4	2.35×10^{-6}	3.79×10^{-6}	2.35×10^{-6}	5.40×10^{-3}	3.72×10^{-3}	5.40×10^{-3}
0.6	3.82×10^{-5}	3.98×10^{-5}	3.82×10^{-5}	2.10×10^{-2}	1.40×10^{-2}	2.10×10^{-2}
0.8	2.72×10^{-4}	2.07×10^{-4}	2.72×10^{-4}	3.60×10^{-2}	3.59×10^{-2}	3.60×10^{-2}
1.0	1.23×10^{-3}	7.38×10^{-4}	1.23×10^{-3}	1.09×10^{-1}	7.49×10^{-2}	1.09×10^{-1}

Table 4. The exact, $E_{Ext_2}^{\alpha=1}(\tau)$ and the residual, $E_{Res_2}^{\alpha=0.5}(\tau)$ errors of $\rho_{2,6}(\tau)$.

	$E_{Ext_2}^{\alpha=1}(\tau)$			$E_{Res_2}^{\alpha=0.5}(\tau)$		
t	LRPST	HAM($\hbar=-1$)	RPST	LRPST	HAM($\hbar=-1$)	RPST
0.0	0	0	0	0	0	0
0.2	2.53×10^{-9}	7.97×10^{-10}	2.53×10^{-9}	2.35×10^{-3}	3.96×10^{-3}	2.35×10^{-3}
0.4	3.24×10^{-7}	1.19×10^{-7}	3.24×10^{-7}	1.99×10^{-2}	3.39×10^{-2}	1.99×10^{-2}
0.6	5.52×10^{-6}	2.40×10^{-6}	5.52×10^{-6}	6.90×10^{-2}	1.20×10^{-1}	6.90×10^{-2}
0.8	4.12×10^{-5}	2.14×10^{-5}	4.12×10^{-5}	1.65×10^{-1}	2.95×10^{-1}	1.65×10^{-1}
1.0	1.95×10^{-4}	1.22×10^{-4}	1.95×10^{-4}	3.26×10^{-1}	5.94×10^{-1}	3.26×10^{-1}

The residual errors, $E_{\ell Res_1}^{\alpha}$ and $E_{\ell Res_2}^{\alpha}$, of the approximation in (38) are defined as:

$$E_{\ell Res_1}^{\alpha} = \left| D^{\alpha}\rho_{1,k}(\tau) + \rho_{1,k}(\tau) + e^{-\tau^{\alpha}}\cos\left(\frac{\tau^{\alpha}}{2}\right)\rho_{2,k}\left(\frac{\tau}{2}\right) + 2e^{-\frac{3\tau^{\alpha}}{4}}\cos\left(\frac{\tau^{\alpha}}{2}\right)\sin\left(\frac{\tau^{\alpha}}{4}\right)\rho_{1,k}\left(\frac{\tau}{4}\right)\right|,$$

$$E_{\ell Res_2}^{\alpha} = \left| D^{\alpha}\rho_{2,k}(\tau) - e^{\tau^{\alpha}}\rho_{1,k}^{2}\left(\frac{\tau}{2}\right) + \rho_{2,k}^{2}\left(\frac{\tau}{2}\right)\right|.$$

The results in the two tables indicate a perfect match between the results of the methods LRPST and RPST, while the new results are much better than those obtained by the HAM method. Also, we can see from the tables that the LRPST solution converges faster to the exact solution. Although the solution resulting from the methods LRPST and RPST are identical, the steps of the solution using the LRPST are easier and faster to reach the required solution.

5. Discussion and conclusions

The main goal of this article is to test the applicability of LRPST to solve the FMPS and to determine its efficiency in creating an accurate solution for it. The results indicate the applicability of the proposed method and provide analytical series solutions for the FMPS that are compatible with the exact solutions. Comparisons of the obtained approximate solutions with those previously obtained by HAM or RPST confirm the efficiency of the presented method. Furthermore, the results we got are consistent with those of RPST. It is worth noting that the calculations used in the LRPST were faster and more straightforward compared to the RPST calculations. This is because it is easier to calculate the limit at infinity compared to calculating the Caputo-fractional derivative that we need many times in each step of the RPST. Accordingly, we conclude that LRPST is a powerful and effective method characterized by simplicity and high accuracy in creating analytical series solutions that converge with accurate FMPS solutions. On the other hand, it can be noted that the software (Mathematica 13) was used in calculating symbolic and numerical quantities in this work and that the time taken for the calculation was short compared to other methods.

As is known, all approximate methods for solving differential equations, whether analytical or numerical, have limits and controls that prevent their application to all equations. The LRPST, like other analytical methods, has conditions when applied that can be summarized in the following points:

- All of the theories related to LRPST are related to Caputo's definition. If it is used to solve fractional DEs with another fractional derivative concept, the theorems in Section 2 must be reformulated to conform to the new characterization.
- All functions used in the DEs to be solved must meet the conditions of the Laplace transform.
- The solution of the target equation plus all its terms must be expandable as a fractional power series.

Therefore, if all these conditions are met in the DE, the LRPST can solve it. Otherwise, the method fails.

Based on the foregoing statement, it can be said that there is a need for more research and work to develop the method used to meet the requirements of other types of differential and integral equations, whether they are fractional or integer orders such as nonlinear diffusion-convection fractional equation [32,52], Klien-Gordon equation, Volterra integral equations [53,54] and other equations [55].

Use of AI tools declaration

The authors declare they have not used Artificial Intelligence (AI) tools in the creation of this article.

Acknowledgments

The authors express their gratitude to the dear referees, who wish to remain anonymous, and the editor for their helpful suggestions.

Conflict of interest

The authors declare no conflict of interest.

References

1. M. A. Matlob, Y. Jamali, The concepts and applications of fractional order differential calculus in modeling of viscoelastic systems: A primer, *Crit. Rev. Biomed. Eng.*, **47** (2019), 249–276. https://doi.org/10.1615/CritRevBiomedEng.2018028368
2. Y. Yu, *Fluid-structure interaction modeling in 3d cerebral arteries and aneurysms*, Biomedical Technology Springer, Cham, 2018, 123–146. https://doi.org/10.1007/978-3-319-59548-1_8
3. C. S. Drapaca, Poiseuille flow of a non-local non-Newtonian fluid with wall slip: A first step in modeling cerebral microaneurysms, *Fractal Frac.*, **6** (2018), 1–9. https://doi.org/10.3390/fractalfract2010009
4. M. A. Yin, A. Yazdani, G. E. Karniadakis, One-dimensional modeling of fractional flow reserve in coronary artery disease: Uncertainty quantification and Bayesian optimization, *Comput. Method. Appl. Mech. Eng.*, **15** (2019), 66–85. https://doi.org/10.1016/j.cma.2019.05.005
5. A. Al-khateeb, H. Zureigat, O. Ala'yed, S. Bawaneh, Ulam-Hyers stability and uniqueness for nonlinear sequential fractional differential equations involving integral boundary conditions, *Fractal Fract.*, **5** (2021), 235. https://doi.org/10.3390/fractalfract5040235
6. X. Li, Y. Sun, Application of RBF neural network optimal segmentation algorithm in credit rating, *Neural Comput. Appl.*, **33** (2021), 8227–8235. https://doi.org/10.1007/s00521-020-04958-9
7. X. Qin, Z. Liu, Y. Liu, S. Liu, B. Yang, L. Yin, et al., User OCEAN personality model construction method using a BP neural network, *Electronics*, **11** (2022), 3022. https://doi.org/10.3390/electronics11193022
8. H. Y. Jin, Z. A. Wang, L. Wu, Global dynamics of a three-species spatial food chain model, *J. Differ. Equ.*, **333** (2022), 144–183. https://doi.org/10.1016/j.jde.2022.06.007
9. H. Y. Jin, Z. A. Wang, L. Wu, Global stabilization of the full attraction-repulsion Keller-Segel system, *Discrete Contin. Dyn. Syst.*, **40** (2020), 3509–3527. https://doi.org/10.3934/dcds.2020027
10. C. C. Hou, T. E. Simos, I. T. Famelis, Neural network solution of pantograph type differential equations, *Math. Method. Appl. Sci.*, **43** (2020), 3369–3374. https://doi.org/10.1002/mma.6126
11. J. Alzabut, A. Selvam, R. A. El-Nabulsi, V. Dhakshinamoorthy, M. E. Samei, Asymptotic stability of nonlinear discrete fractional pantograph equations with non-local initial conditions, *Symmetry*, **13** (2021), 473. https://doi.org/10.3390/sym13030473
12. M. Arnold, B. Simeon, Pantograph and catenary dynamics: A benchmark problem and its numerical solution, *Appl. Numer. Math.*, **34** (2000), 345–362. https://doi.org/10.1016/S0168-9274(99)00038-0
13. W. G. Ajello, H. I. Freedman, J. Wu, A model of stage structured population growth with density depended time delay, *SIAM J. Appl. Math.*, **52** (1992), 855–869. https://doi.org/10.1137/0152048
14. M. D. Buhmann, A. Iserle, Stability of the discretized pantograph differential equation, *J. Math. Comput.*, **60** (1993), 575–589. https://doi.org/10.1090/S0025-5718-1993-1176707-2
15. J. R. Ockendon, A. B. Tayler, The dynamics of a current collection system for an electric locomotive, *Proc. R. Soc. Lond. Ser. A*, **322** (1971), 447–468. https://doi.org/10.1098/rspa.1971.0078
16. S. Widatalla, M. A. Koroma, Approximation algorithm for a system of pantograph equations, *J. Appl. Math.*, **2012** (2012), 1–9. https://doi.org/10.1155/2012/714681

17. D. Li, M. Z. Liu, Runge-Kutta methods for the multi-pantograph delay equation, *Appl. Math. Comput.*, **163** (2005), 383–395. https://doi.org/10.1016/j.amc.2004.02.013
18. M. Sezer, N. Şahin, Approximate solution of multi-pantograph equation with variable coefficients, *J. Comput. Appl. Math.*, **214** (2008), 406–416. https://doi.org/10.1016/j.cam.2007.03.024
19. M. Z. Liu, D. Li, Properties of analytic solution and numerical solution of multi-pantograph equation, *Appl. Math. Comput.*, **155** (2004), 853–871. https://doi.org/10.1016/j.amc.2003.07.017
20. C. Yang, Modified Chebyshev collocation method for pantograph-type differential equations, *Appl. Numer. Math.*, **134** (2018), 132–144. https://doi.org/10.1016/j.apnum.2018.08.002
21. Z. Avazzadeh, M. H. Heydari, M. R. Mahmoudi, An approximate approach for the generalized variable-order fractional pantograph equation, *Alex. Eng. J.*, **59** (2020), 2347–2354. https://doi.org/10.1016/j.aej.2020.02.028
22. M. S. Hashemi, E. Ashpazzadeh, M. Moharrami, M. Lakestani, Fractional order Alpert multiwavelets for discretizing delay fractional differential equation of pantograph type, *Appl. Numer. Math*., **170** (2021), 1–13. https://doi.org/10.1016/j.apnum.2021.07.015
23. S. S. Ezz-Eldien, On solving systems of multi-pantograph equations via spectral tau method, *Appl. Math. Comput.*, **321** (2018), 63–73. https://doi.org/10.1016/j.amc.2017.10.014
24. Ş. Yüzbaşı, An efficient algorithm for solving multi-pantograph equation systems, *Appl. Math. Comput.*, **64** (2012). 589–603. https://doi.org/10.1016/j.camwa.2011.12.062
25. R. Saadeh, A reliable algorithm for solving system of multi-pantograph equations, *WSEAS Trans. Math.*, **21** (2022), 792–800. https://doi.org/10.37394/23206.2022.21.91
26. O. Mohammed, H. Salim, Computational methods based Laplace decomposition for solving nonlinear system of fractional order differential equations, *Alex. Eng. J.*, **57** (2018), 3549–3557. https://doi.org/10.1016/j.aej.2017.11.020
27. M. Zurigat, Solving Fractional oscillators using Laplace homotopy analysis method, *Ann. Univ. Craiova Math. Comput.*, **38** (2011), 1–11.
28. J. Prakash, M. Kothandapani, V. Bharathi, Numerical approximations of nonlinear fractional differential difference equations by using modified He-Laplace method, *Alex. Eng. J.*, **55** (2016), 645–651. https://doi.org/10.1016/j.aej.2015.12.006
29. A. El-Ajou, Adapting the Laplace transform to create solitary solutions for the nonlinear time-fractional dispersive PDEs via a new approach, *Eur. Phys. J. Plus.*, **136** (2021), 229. https://doi.org/10.1140/epjp/s13360-020-01061-9
30. T. Eriqat, A. El-Ajou, M. N. Oqielat, Z. Al-Zhour, S. Momani, A new attractive analytic approach for solutions of linear and nonlinear neutral fractional pantograph equations, *Chaos Soliton. Fract.*, **138** (2020), 109957. https://doi.org/10.1016/j.chaos.2020.109957
31. R. Saadeh, A. Burqan, A. El-Ajou, Reliable solutions to fractional Lane-Emden equations via LT and residual error function, *Alex. Eng. J.*, **61** (2022), 10551–10562. https://doi.org/10.1016/j.aej.2022.04.004
32. E. Salah, A. Qazza, R. Saadeh, A. El-Ajou, A hybrid analytical technique for solving multi-dimensional time-fractional Navier-Stokes system, *AIMS Math.*, **8** (2023), 1713–1736. https://doi.org/10.3934/math.2023088
33. T. Eriqat, M. Oqielat, Z. Al-Zhour, A. El-Ajou, A. Bataineh, Revisited Fisher's equation and logistic system model: A new fractional approach and some modifications, *Int. J. Dyn. Control.*, **2022** (2022). https://doi.org/10.1007/s40435-022-01020-5
34. T. Humphries, *Delay differential equations*, In: 2016 NZMRI Summer School Continuation Methods in Dynamical Systems Raglan, New Zealand, 2016.

35. R. Saadeh, A. Qazza, K. Amawi, A new approach using integral transform to solve cancer models, *Fractal Fract.*, **6** (2022), 490. https://doi.org/10.3390/fractalfract6090490
36. B. K. Singh, S. Agrawal, Study of time fractional proportional delayed multi-pantograph system and integro-differential equations, *Math. Method. Appl. Sci.*, **45** (2022), 8305–8328. https://doi.org/10.1002/mma.8335
37. Z. Gong, C. Liu, K. L. Teo, X. Yi, Optimal control of nonlinear fractional systems with multiple pantograph-delays, *Appl. Math. Comput.*, **425** (2022), 127094. https://doi.org/10.1016/j.amc.2022.127094
38. M. Inc, The approximate and exact solutions of the space- and time-fractional Burgers equations with initial conditions by variational iteration method, *J. Math. Anal. Appl.*, **345** (2008), 476–484. https://doi.org/10.1016/j.jmaa.2008.04.007
39. S. Hasan, A. El-Ajou, S. Hadid, M. Al-Smadi, S. Momanid, Atangana-Baleanu fractional framework of reproducing kernel technique in solving fractional population dynamics system, *Chaos Soliton. Fract.*, **133** (2020), 109624. https://doi.org/10.1016/j.chaos.2020.109624
40. S. Ray, R. K. Bera, An approximate solution of a nonlinear fractional differential equation by Adomian decomposition method, *Appl. Math. Comput.*, **167** (2005), 561–571. https://doi.org/10.1016/j.amc.2004.07.020
41. Y. Zhang, A finite difference method for fractional partial differential equation, *Appl. Math. Comput.*, **215** (2009), 524–529. https://doi.org/10.1016/j.amc.2009.05.018
42. Q. Wang, Homotopy perturbation method for fractional KdV-Burgers equation, *Chaos Soliton. Fract.*, **35** (2008), 843–850. https://doi.org/10.1016/j.chaos.2006.05.074
43. I. Hashim, O. Abdulaziz, S. Momani, Homotopy analysis method for fractional IVPs, *Commun. Nonlinear Sci.*, **14** (2009), 674–684. https://doi.org/10.1016/j.cnsns.2007.09.014
44. H. Rezazadeh, S. M. Mirhosseini-Alizamini, A. Neirameh, A. Souleymanou, A. Korkmaz, A. Bekir, Fractional Sine-Gordon equation approach to the coupled higgs system defined in time-fractional form, *Iran. J. Sci. Technol. A*, **43** (2019), 2965–2973. https://doi.org/10.1007/s40995-019-00780-8
45. A. Jafarian, M. Mokhtarpour, D. Baleanu, Artificial neural network approach for a class of fractional ordinary differential equation, *Neural. Comput. Appl.*, **28** (2017), 765–773. https://doi.org/10.1007/s00521-015-2104-8
46. A. El-Ajou, M. Oqielat, Z. Al-Zhour, S. Momani, A class of linear non-homogenous higher order matrix fractional differential equations: analytical solutions and new technique, *Fract. Calc. Appl. Anal.*, **23** (2020), 356–377. https://doi.org/10.1515/fca-2020-0017
47. A. El-Ajou, Taylor's expansion for fractional matrix functions: Theory and applications, *J. Math. Comput. Sci.*, **21** (2020), 1–17. https://doi.org/10.22436/jmcs.021.01.01
48. A. Burqan, R. Saadeh, A. Qazza, S. Momani, ARA-residual power series method for solving partial fractional differential equations, *Alex. Eng. J.*, **62** (2022), 47–62. https://doi.org/10.1016/j.aej.2022.07.022
49. D. V. Widder, *Laplace transform (PMS-6)*, Princeton University Press, **64** (2015).
50. A. Qazza, R. Saadeh, On the analytical solution of fractional SIR epidemic model, *Appl. Comput. Intell. Soft Comput.*, **2023** (2023). https://doi.org/10.1155/2023/6973734
51. I. Podlubny, *Fractional differential equations*, Academic Press, San Diego, 1999.
52. E. Salah, R. Saadeh, A. Qazza, R. Hatamleh, Direct power series approach for solving nonlinear initial value problems, *Axioms*, **12** (2023), 111. https://doi.org/10.3390/axioms12020111
53. A. Qazza, Solution of integral equations via Laplace ARA transform, *Eur. J. Pure Appl. Math.*, **16** (2023), 919–933. https://doi.org/10.29020/nybg.ejpam.v16i2.4745

54. R. Saadeh, A generalized approach of triple integral transforms and applications, *J. Math.*, **2023** (2023). https://doi.org/10.1155/2023/4512353
55. R. Luo, Z. Peng, J. Hu, On model identification based optimal control and it's applications to multi-agent learning and control, *Mathematics*, **11** (2023), 906. https://doi.org/10.3390/math11040906